

Preparation, Characteristics, and Stability of Glutathione-Loaded Nanoparticles

Seung Hyun Koo,[†] Ji-Soo Lee,[†] Gun-Hee Kim,[‡] and Hyeon Gyu Lee^{*,†}

[†]Department of Food and Nutrition, Hanyang University, 17 Haengdang-dong, Seongdong-gu, Seoul 133-791, Republic of Korea

[‡]Plant Resources Research Institute, Duksung Women's University, 419 Ssangmun-dong, Dobong-gu, Seoul 132-174, Republic of Korea

ABSTRACT: The aim of this study was to investigate the characteristics and oxidative stability of chitosan–glutathione conjugate (CS–GSH) and CS–GSH nanoparticles (CS–GSH NPs) to explore the potentials of these nanoparticle systems for GSH delivery. CS–GSH was synthesized using a radical polymerization method, and CS–GSH NP was prepared by ionic gelation of CS–GSH with sodium tripolyphosphate (TPP). The sizes of CS–GSH NPs significantly increased with increasing CS–GSH concentration and CS–GSH/TPP ratio. The entrapment efficiency (EE) significantly increased with increasing CS–GSH concentration and significantly decreased with increasing CS–GSH/TPP ratio. The immobilized GSH could be protected against oxidation compared to free GSH. The thiol content in the nanoencapsulated GSH was more effectively maintained than those in free GSH and CS–GSH, regardless of the presence of oxidative stress-inducing agents. These results suggest that CS–GSH NP can be used to enhance the oxidative stability of GSH.

KEYWORDS: glutathione, chitosan, thiolated chitosan, nanoparticle, stability

INTRODUCTION

Glutathione (γ -glutamylcysteinylglycine, GSH), the most abundant cellular thiol and nucleophilic tripeptide, is of great interest due to its roles in various enzymatic and nonenzymatic detoxification mechanisms.¹ As a scavenger of free radicals, GSH can protect cells against reactive oxygen species and xenobiotics.² GSH can also protect organs, such as the kidney, liver, lung, and intestine, which are frequently exposed to xenobiotics.³ A decreased GSH level is associated with aging and various diseases, including cataracts, hemolysis, alcoholic liver injury, diabetes mellitus, and cancer.^{4,5}

However, the application of GSH as a functional food ingredient has been limited because of its low bioavailability due to its poor cellular uptake¹ and its instability in neutral or alkaline environments. Under conditions of oxidative stress, the GSH thiol group can be easily oxidized to glutathione disulfide (GSSG), which loses its antioxidant activity based on its radical scavenging activity.⁶

Encapsulation systems have been used to protect sensitive ingredients as a delivery mechanism during food processing and storage against environmental conditions such as light, oxygen, water, and temperature.^{7,8} In addition, encapsulation has been applied to improve the functionality and bioavailability of bioactive materials.⁹ Recently, nanoparticle (NP) systems have been progressively used as delivery systems for various natural bioactive materials.^{10,11} The NP system provides a polymeric barrier for the core materials against the oxidative conditions, resulting in improvement of the stability. In addition, the NP system is capable of improving bioavailability, due to increased water dispersibility and direct NP cellular uptake.^{12,13}

A few delivery systems have been developed for GSH in recent years. GSH can be protected against chemical or enzymatic degradation by microencapsulation.¹⁴ Gate et al.¹ used a liposomal-encapsulated system to replenish depleted intracellular GSH.

Atyabi et al.¹⁵ developed polyhydroxyethyl methacrylate NPs coated by thiolated chitosan and evaluated their physical characteristics, including particle size, polydispersity index, and zeta potential. However, little progress has been reported on a NP delivery system for GSH to improve its stability.

Chitosan, a polymer of β -(1 \rightarrow 4)-linked 2-amino-2-deoxy-D-glucopyranose, has been widely used for the oral delivery of many bioactive proteins and drugs. Chitosan NPs can be easily produced by ionic gelation between cationic amino groups of chitosan and multivalent anions, such as tripolyphosphate (TPP).¹⁶ Chitosan nanodelivery systems are very useful in drug delivery applications due to their nontoxic, biodegradable, biocompatible, and mechanically strong properties.¹⁷ Other advantages include their improved bioadhesibility and water dispersibility; therefore, they can provide incorporated bioactive substances with a much longer gastrointestinal tract residence time, resulting in improved bioavailability. Therefore, it seems reasonable to hypothesize that chitosan could be an appropriate nanocarrier for GSH.^{15,18–21} Especially, the CS–GSH conjugate by direct immobilization of GSH on CS can be available for the delivery system for enhancing stability and bioavailability of GSH; however, there is little information about a NP system using CS–GSH.

The aim of this study was to investigate the characteristics and stability of CS–GSH and CS–GSH NPs to explore their potentials as nanoparticle systems for GSH. Therefore, (1) CS–GSH was synthesized by the immobilization of GSH on chitosan, (2) CS–GSH NPs were prepared by an ionic gelation reaction of CS–GSH with TPP anions, (3) characteristics such

Received: June 21, 2011

Revised: September 2, 2011

Accepted: September 2, 2011

Published: September 02, 2011

as particle size, entrapment efficiency, and loading efficiency of CS–GSH NPs were investigated, and (4) the stability of CS–GSH and CS–GSH NPs was evaluated.

MATERIALS AND METHODS

Materials. Chitosan with a deacetylation degree of 86.6% and a low molecular weight (50–190 kDa) was purchased from Sigma-Aldrich Chemical Co. (Sigma, St. Louis, MO). Reduced glutathione (GSH), 1-ethyl-3-(3-dimethylaminopropyl) carbodiimide hydrochloride (EDAC), *N*-hydroxysuccinimide (NHS), *L*-cysteine hydrochloride anhydrous, sodium borohydride, 5,5'-dithiobis(2-nitrobenzoic acid), and TPP were also purchased from Sigma-Aldrich. All other reagents were of analytical grade.

Preparation of the CS–GSH Conjugate. Preparation of CS–GSH was performed according to the method of Kafedjiiski et al.²² with some modification. In brief, 0.3 g of chitosan was hydrated in 2.4 mL of 1 M HCl and dissolved by the addition of distilled water to obtain a 1% (w/v) polymer solution. The chitosan solution was adjusted to pH 6.0 with 5 M NaOH, and then 2.4 mL of the GSH solution (250 mg/mL) was added to the chitosan solution (12 mL) under continuous magnetic stirring. Then, the EDAC and NHS solutions were sequentially added into the reaction mixture under magnetic stirring to a final concentration of 200 mM. The pH was readjusted to 6.0 with 5 M NaOH. Under magnetic stirring, the reaction mixture was incubated for 15 h at room temperature. The reaction mixture was dialyzed in 12 kDa molecular weight cutoff tubing first against 5 mM HCl, twice against 5 mM HCl containing 1% NaCl, and finally twice against 1 mM HCl. Controls were prepared in the same way, but EDAC and NHS were omitted. Finally, samples and controls were lyophilized and stored at –80 °C before further analyses.

Preparation of CS–GSH NPs. CS–GSH NPs were obtained by inducing the ionic gelation of CS–GSH with TPP anions.²³ CS–GSH was dissolved in distilled water at final concentrations of 0.5, 1.0, and 1.5 mg/mL. Under magnetic stirring (1000 rpm) at room temperature, 4 mL of TPP solution (0.1–0.38 mg/mL) was dropped into 4 mL of CS–GSH solution using a cassette tube pump (EYELA SMP-21, Tokyo Rikakikai Co. Ltd., Tokyo, Japan) at a drop rate of 1 min/mL.

Determination of Thiol Group Content. The amounts of free thiol groups in CS–GSH and CS–GSH NPs were measured spectrophotometrically using Ellman's reagent as described by Habeeb²⁶ and Bernkop-Schnrch et al.²⁴ with modification. Briefly, 0.25 mL of sample solution, 0.125 mL of 1 M phosphate buffer (pH 8.0), and 50 μ L of 0.3% Ellman's reagent (dissolved 0.5 M phosphate buffer of pH 8.0) were mixed and left for 2 h at room temperature. After centrifugation (24000g, 5 min), 200 μ L of the supernatant was transferred to a 96-well plate. Immediately, the absorbance was measured at 450 nm with a universal microplate reader (ELx800 uv, Bio-Tek Instrument Inc., Winooski, VT). To calculate the number of sulfhydryl groups immobilized on the polymer, the cysteine hydrochloride was used as a standard.

The total amount of sulfhydryl groups in CS–GSH and CS–GSH NPs was represented by the summation of reduced free thiol groups and oxidized thiol groups in the form of disulfide bonds and measured according to the method described by Guggi and Bernkop-Schnrch.²⁵ In brief, 0.5 mg of sample was suspended in 1 mL of 0.05 M tris-(hydroxymethyl)aminomethane buffer (pH 6.8). After 30 min, 1 mL of an 8% sodium borohydride solution was added to the polymer solution. The mixture was incubated for 1 h in a shaking water bath at 37 °C. To remove the remaining sodium borohydride, the mixture was agitated for 10 min by the addition of 200 μ L of 5 M HCl. Then, 1 mL of 1 M phosphate buffer (pH 8.5) was added until neutralization, and immediately 100 μ L of 0.4% Ellman's reagent was mixed. After reaction for 15 min at room temperature, the mixture was transferred to a 96-well plate, and the absorbance was measured at 450 nm using a universal

microplate reader. Disulfide content was calculated by subtracting the quantity of free thiol groups from the number of total thiol groups.

Particle Size Measurement of CS–GSH NPs. The sizes of CS–GSH NPs were measured by quasielastic laser light scattering using a Delsa Nano C instrument (Beckman Coulter Inc., Fullerton, CA) at 25 \pm 1 °C. Triplicate samples were measured, and the arithmetic mean value of the three was adopted.

Entrapment and Loading Efficiencies of CS–GSH NPs. The entrapment efficiencies (EE) and loading efficiencies (LE) of CS–GSH NPs were determined by separation from NP suspensions using ultracentrifugation (Optima TL ultracentrifuge, Beckman, Fullerton, CA) at 42000g for 50 min.²³ The thiol group content entrapped within the NPs was determined by measuring nonentrapped thiol groups in the supernatant. The EE and LE of the CS–GSH NPs were calculated using the following formulas:

$$EE (\%) = \frac{\text{actual amount of GSH entrapped in NPs}}{\text{theoretical amount of GSH entrapped in NPs}} \times 100 \quad (1)$$

$$LE (\%) = \frac{\text{actual amount of GSH entrapped in NPs}}{\text{weight of NPs}} \times 100 \quad (2)$$

Transmission Electron Microscopy (TEM). TEM (LEO 912AB, Carl Zeiss Inc., Germany) was used to observe the morphology of CS–GSH NPs. A drop of NP suspension was dried on a copper grid, and then the sample was negatively stained with a 2% phosphotungstic acid aqueous solution (pH 7.4) for 30 min before analysis.

Stability of CS–GSH NPs. The stabilities of free GSH, CS–GSH, and CS–GSH NPs were estimated by measuring thiol group content. Free GSH and CS–GSH solutions were respectively adjusted to pH 5.4, which is the pH value found in the CS–GSH NP dispersion. All tested samples were incubated at 25 °C for 16 days. In addition, changes in the thiol group contents of GSH, CS–GSH, and CS–GSH NP were measured after the addition of 20 μ L of H₂O₂ (8–33 μ g/mL) as the oxidative agent.

Statistical Analysis. Statistical analyses were conducted using SPSS (Statistical Package for the Social Sciences, SPSS Inc., Chicago, IL). One-way analyses of variance (ANOVA) were performed ($p < 0.05$). All experiments were performed at least in triplicate, and results are presented as the mean \pm standard deviation (SD).

RESULTS AND DISCUSSION

Characterization of CS–GSH. CS–GSH was synthesized by the formation of an amide bond between the chitosan amino group (NH₂) and the glycine carboxyl group (COOH) in glutathione.^{20,22} EDAC was used for the coupling reaction of chitosan and glutathione. After carboxylic acid groups of GSH were activated to *O*-acylisourea groups by EDAC, *O*-acylisourea groups were converted into a NHS-activated carboxylic acid groups, resulting in cross-links between activated carboxylic acid groups and amine groups of chitosan. In addition, NHS was used to improve EDAC-mediated coupling reaction yields.²² The obtained CS–GSH appeared as a white, odorless powder and was solubilized in distilled water to make a transparent, low-viscosity solution. The amounts of immobilized free thiol groups and disulfide bonds in CS–GSH were determined to be 111 and 535 μ mol/g polymer, respectively. No thiol group was detected in the control polymer prepared without EDAC and NHS, indicating that the purification step of five consecutive dialyses was efficient. Our results for the free thiol and disulfide bond contents of CS–GSH were similar to the results (93 and 595 μ mol/g polymer, respectively) reported by Akhlaghi et al.,²⁶ who

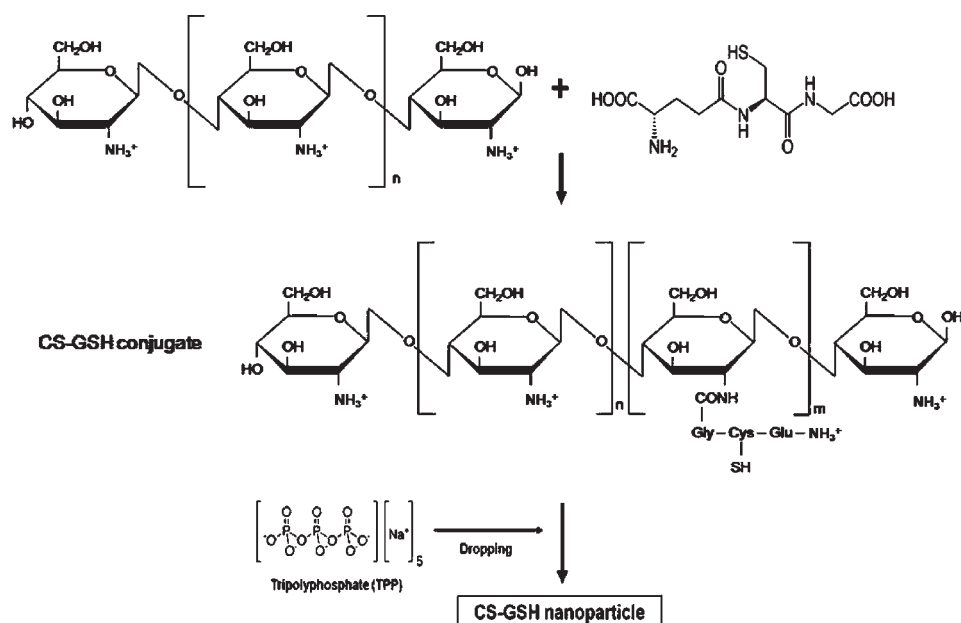


Figure 1. Scheme for CS–GSH NP preparation.

immobilized GSH on the low molecular weight chitosan. However, Kafedjiiski et al.²² reported that in conjugates with medium molecular weight chitosan, the free thiol and disulfide bond contents were found to be 266 and 398 $\mu\text{mol/g}$ polymer, respectively, which were 2-fold higher than our results. This difference could be because of the molecular weights of chitosan. According to Atyabi et al.,¹⁵ the CS–GSH with lower molecular weight chitosan exhibited fewer free thiol groups and more disulfide bonds, because in low molecular weight chitosan, GSH is immobilized in closer positions and inter- and intramolecular disulfide bonds can be formed.

Physicochemical Properties of CS–GSH NPs. The CS–GSH NPs were prepared by the addition of TPP anions. It was expected that CS-based NPs would be formed via ionic gelation between the positively charged amino groups of CS and the negatively charged TPP. However, it is probable that the amino group of the GSH moiety in CS–GSH conjugate also ionically interacted with TPP anions, although further investigations are necessary to identify the ionic gelation mechanism of CS–GSH conjugate. The scheme for the preparation of CS–GSH NPs is shown Figure 1. The effects of chitosan concentration and CS–GSH/TPP ratio on the particle size and the polydispersity index (PDI) of CS–GSH NPs were investigated (Table 1). The size of CS–GSH NPs prepared by different conditions ranged from 168 to 486 nm. The sizes of CS–GSH NPs significantly increased with increasing CS–GSH concentrations at a fixed CS–GSH/TPP ratio. These results can be explained as follows: during the formation of CS–GSH NPs, the viscosity of the stirred solution was higher at the increased chitosan concentrations, resulting in large particle size distribution.^{27,28} In addition, the particle size significantly increased with the increase in CS–GSH/TPP ratio, which can be explained by the fact that at the higher TPP concentrations, the cross-linking of chitosan NP was induced by the higher electrostatic interaction, resulting in a more compact NP structure.²⁹

PDI is defined as the particle size distribution of the nanoparticles (in particular, the width of the distribution). The values of PDI close to 0 exhibited a homogeneous dispersion, whereas

Table 1. Physicochemical Properties of CS–GSH NPs

CS–GSH (mg/mL)	CS–GSH/TPP ratio	particle size ^a (nm)	polydispersity index
0.5	6	168.22 ± 13.78 d	0.228 ± 0.048
	8	199.67 ± 24.91 d	0.173 ± 0.037
	10	254.59 ± 59.02 cd	0.168 ± 0.050
1.0	6	195.12 ± 22.99 d	0.254 ± 0.046
	8	275.62 ± 68.76 cd	0.247 ± 0.036
	10	351.87 ± 50.41 bc	0.237 ± 0.056
	12	406.86 ± 136.23 ab	0.200 ± 0.049
1.5	8	293.32 ± 27.49 bcd	0.307 ± 0.030
	10	401.27 ± 66.21 ab	0.248 ± 0.029
	12	486.37 ± 97.78 a	0.269 ± 0.064

^a Means with different letters (a–d) indicate a significant difference between them ($p < 0.05$).

those >0.3 exhibited high heterogeneity.³⁰ PDI values of CS–GSH NPs prepared in this study were not significantly different at various CS–GSH concentrations and CS–GSH/TPP ratios and ranged from 0.2 to 0.3. Therefore, the results indicate that a homogeneous dispersion of CS–GSH NPs was obtained regardless of the CS–GSH concentration and the CS–GSH/TPP ratio.

Entrapment and Loading Efficiencies of CS–GSH NPs. To investigate the effect of chitosan concentration and CS–GSH/TPP ratio on the EE and LE of CS–GSH NPs, EE and LE were measured by comparing the free thiol group content before and after nanoencapsulation. The EE increased with CS–GSH concentration at a fixed CS–GSH/TPP ratio (Figure 2). As mentioned above, the high viscosity of the CS–GSH solution at a high concentration could decrease the extent of GSH diffusion into gelling medium during NP formation, leading to greater EE. In addition, the EE significantly decreased with CS–GSH/TPP

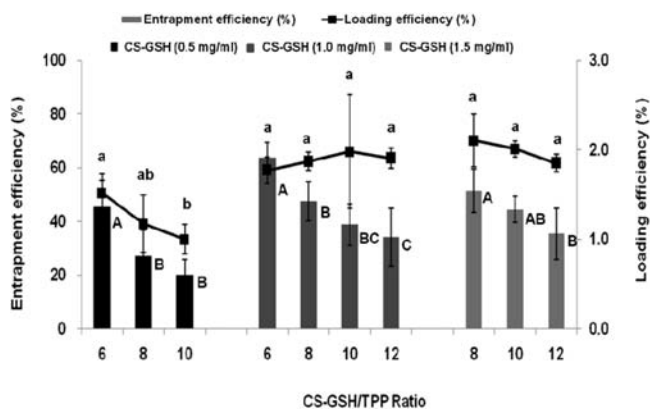


Figure 2. Entrapment and loading efficiencies of CS–GSH NPs with different CS–GSH concentrations and CS/TPP ratios. Different capital letters (A–C) on the bars indicate a significant difference in entrapment efficiency (EE) ($p < 0.05$). Different small letters (a, b) on the lines indicate a significant difference in loading efficiency (LE) ($p < 0.05$).

ratio. This result could be explained due to the fact that the denser TPP-mediated CS–GSH network structure forming at a lower CS/TPP ratio may reduce diffusional loss of GSH out of CS–GSH NP during the preparation procedure, resulting in a higher EE.^{28,31} As the CS–GSH/TPP ratio was increased from 6 to 10 at CS–GSH concentration of 0.5 mg/mL, the LE of CS–GSH NPs significantly decreased (Figure 2). However, as the CS–GSH concentration was increased from 1.0 to 1.5 mg/mL, the LE of CS–GSH NPs did not show a significant difference. This could be attributed to the fact that as the CS–GSH/TPP ratio increased, the available quantity of TPP decreased accordingly, and the weight of CS–GSH NPs obtained by ultracentrifugation decreased. This tendency was clearly observed at high CS–GSH concentration. Because LE was calculated as the weight of GSH entrapped in NPs to the weight of NPs, the effect of CS–GSH/TPP ratio on the LE did not appear at a high CS–GSH concentration. The optimized NP preparation conditions were determined as 1.5 mg/mL CS–GSH and a CS–GSH/TPP ratio of 8, because of the highest LE, even though without significant difference. The particle size prepared according to the optimum conditions was found to be 293 nm. According to Akhlaghi et al.,²⁶ NP size is one of the most important determinants in cellular uptake and a particle size of >500 nm decreases the permeability of the particles through the intestinal mucosa.

Morphology of CS–GSH NPs. TEM analysis confirmed the presence of NPs and revealed their morphological properties. In TEM images of CS–GSH NPs prepared under the optimized conditions (Figure 3), the NPs showed a dense and spherical structure that ranged from approximately 140 to 290 nm, which is considerably smaller than the particle size obtained from DLS. This apparent discrepancy can be explained by two reasons: first, TEM measures the dried particle size during sample preparation and, second, DLS measures the particle size including the electrical double layer that surrounds a particle.

Stability of CS–GSH NPs. To investigate NP stability, GSH, CS–GSH, and CS–GSH NPs were stored at 25 °C for 16 days and their thiol contents were evaluated. The low H^+ concentration in a high-pH environment forces thiol groups to form intra- and intermolecular disulfide bonds, and the oxidation of the immobilized free thiol groups can also be influenced by the pH

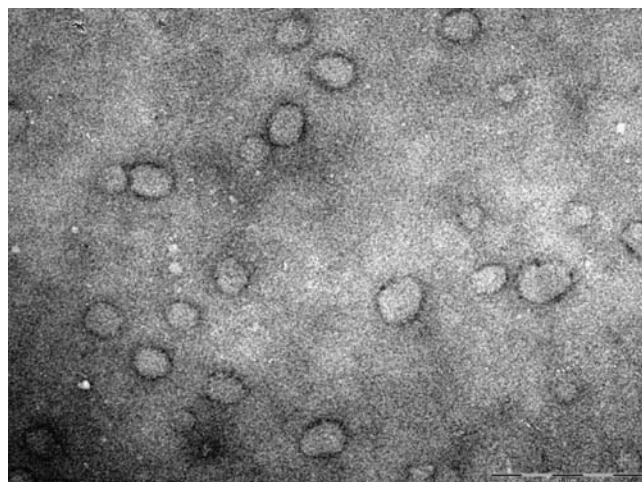


Figure 3. Transmission electron micrograph of a CS–GSH NP prepared under the optimized conditions (1.5 mg/mL CS–GSH and a CS–GSH/TPP ratio of 8). The scale bar represents a distance of 1 μ m.

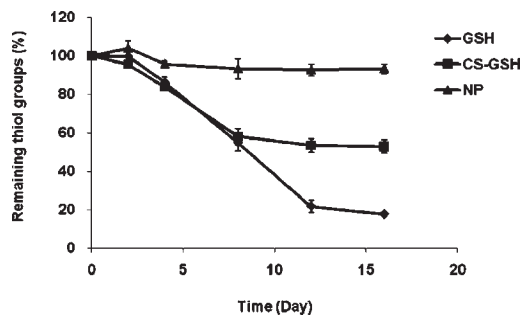


Figure 4. Decrease in thiol group content within GSH, CS–GSH, and CS–GSH NPs at 0.03 mg/mL concentration, pH 5.4, and 25 °C.

value.^{24,32,33} Therefore, to exclude the effects of pH on the stability of GSH, the pH values of free GSH and CS–GSH solutions were adjusted to 5.4, which is the pH value found in CS–GSH NP dispersions. As shown in Figure 4, as storage time increased, the thiol content of free GSH rapidly decreased to reach about 18% on day 16. The thiol content of CS–GSH also rapidly decreased until day 8; after this time, its remaining thiol content was maintained at about 55%. However, after slightly decreasing until day 4, thiol groups of the CS–GSH NPs were maintained at approximately 94%. These results can be explained as follows: free GSH is susceptible to oxidation because of disulfide bond formation; however, when GSH was immobilized on chitosan, the GSH can be partially protected against oxidation. In addition, as GSH was nanoencapsulated, the free thiol groups could be doubly protected by the immobilization of GSH on chitosan and by nanoparticulation via ionic gelation between CS with TPP.

To investigate the stability of GSH, CS–GSH, and CS–GSH NPs under oxidative stress, the effect of the presence of H_2O_2 on their thiol contents was evaluated. As shown in Figure 5, the thiol group contents of all samples tested in this study decreased with the addition of H_2O_2 . With respect to stability, reduction of free GSH was significantly greatest with observed reductions in CS–GSH and CS–GSH NPs in subsequent order. In particular, the thiol content of the CS–GSH NPs was about 1.5-fold higher than that of free GSH. These results were

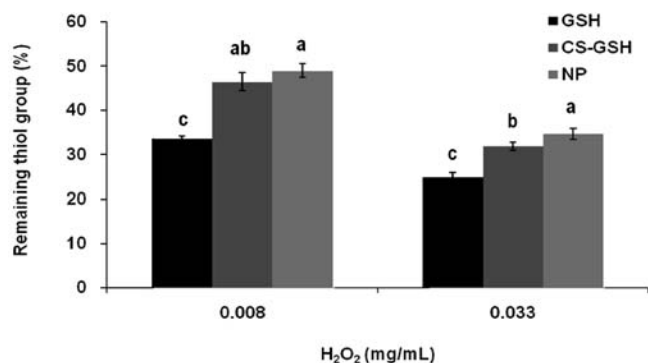


Figure 5. Decrease in thiol group content within GSH, CS-GSH, and CS-GSH NPs with the addition of H₂O₂ (20 μ L). Different letters (a–c) on the bars indicate significant difference ($p < 0.05$).

similar to our previous stability results, indicating that the GSH protection effect was induced by immobilization and that nanoencapsulated GSH can be more effectively maintained under oxidative stress. These results clearly demonstrate that the oxidative stability of GSH can be improved by CS-GSH nanoencapsulation from the oxidative environment. Therefore, CS-GSH NPs could be used as an effective delivery carrier to improve the oxidative stability of GSH in the food industry.

AUTHOR INFORMATION

Corresponding Author

*Phone: +82-2-2220-1202. Fax: +82-2-2281-8285. E-mail: hyeonlee@hanyang.ac.kr.

Funding Sources

This work was supported by Priority Research Centers Program through the National Research Foundation of Korea (NRF) funded by the Ministry of Education, Science and Technology (2010-0029692).

REFERENCES

- Gate, L.; Vauthier, C.; Couvreur, P.; Tew, K. D.; Tapiero, H. Glutathione-loaded poly(isobutylcyanoacrylate) nanoparticles and liposomes: comparative effects in murine erythrocytopenia and macrophage-like cells. *STP Pharm. Sci.* **2011**, *11*, 355–361.
- Meister, A. Glutathione deficiency produced by inhibition of its synthesis and its reversal: applications in research and therapy. *Pharmacol. Ther.* **1991**, *51*, 155–194.
- Deleve, L. D.; Kaplowitz, N. Glutathione metabolism and its role in hepatotoxicity. *Pharmacol. Ther.* **1991**, *52*, 287–305.
- Flagg, E. W.; Coates, R. J.; Jones, D. P.; Byers, T. E.; Greenberg, R. S.; Gridkey, G.; Mclaughlin, J. K.; Blot, W. J.; Haber, M.; Preston-Martin, S. Dietary glutathione intake and risk of oral and pharyngeal cancer. *Am. J. Epidemiol.* **1994**, *139*, 453–465.
- Lu, S. C. Regulation of glutathione synthesis. *Mol. Aspects Med.* **2009**, *30*, 42–59.
- Camera, E.; Picardo, M. Analytical methods to investigate glutathione and related compounds in biological and pathological processes. *J. Chromatogr. B* **2002**, *781*, 181–206.
- Dziedzic, J. D. Microcapsulation and encapsulated ingredients. *Food Technol.* **1998**, *42*, 136–151.
- Risch, S. J. *Encapsulation and Controlled Release of Food Ingredients*; ACS Symposium Series 590; American Chemical Society: Washington, DC, 1995; pp 2–7.

(9) Pothakamury, U. R.; Barbosa-Canovas, G. V. Fundamental aspects of controlled release in foods. *Trends Food Sci. Technol.* **1995**, *6*, 397–406.

(10) Opanasopit, P.; Apirakaramwong, A.; Ngawhirunpat, T.; Rojanarata, T.; Ruktanonchai, U. Development and characterization of pectinate micro/nanoparticles for gene delivery. *AAPS Pharm. Sci. Technol.* **2008**, *9*, 67–74.

(11) Sanguansri, P.; Augustin, M. A. Nanoscale materials development – a food industry perspective. *Trends Food Sci. Technol.* **2006**, *17*, 547–556.

(12) Pinto Reis, C.; Neufeld, R. J.; Ribeiro, A. I. J.; Veiga, F. Nanocapsulation II. Biomedical applications and current status of peptide and protein nanoparticulate delivery systems. *Nanomed.—Nanotechnol.* **2006**, *2*, 53–65.

(13) Acosta, E. Bioavailability of nanoparticles in nutrient and nutraceutical delivery. *Curr. Opin. Colloid Interface Sci.* **2009**, *14*, 3–15.

(14) Trapani, A.; Laquintana, V.; Denora, N.; Lopodota, A.; Cutrignelli, A.; Franco, M.; Trapani, G.; Liso, G.; Eudragit, R. S. 100 microparticles containing 2-hydroxypropyl- β -cyclodextrin and glutathione: physicochemical characterization, drug release and transport studies. *Eur. J. Pharm. Sci.* **2007**, *30*, 65–74.

(15) Atyabi, F.; Moghaddam, F. A.; Dinarvand, R.; Zohuriaan-Mehr, M. Z.; Ponchel, G. Thiolated chitosan coated poly hydroxyethyl methacrylate nanoparticles: synthesis and characterization. *Carbohydr. Polym.* **2008**, *74*, 59–67.

(16) Lin, Y. H.; Chung, C. K.; Chen, C. T.; Liang, H. F.; Chen, S. C.; Sung, H. W. Preparation of nanoparticles composed of chitosan/poly- γ -glutamic acid and evaluation of their permeability through Caco-2 cells. *Biomacromolecules* **2005**, *6*, 1104–1112.

(17) Agnihotri, S. A.; Mallikarjuna, N. N.; Aminabhavi, T. M. Recent advances on chitosan-based micro- and nanoparticles in drug delivery. *J. Controlled Release* **2004**, *100*, 5–28.

(18) Guggi, D.; Kast, C. E.; Bernkop-Schnurch, A. In vivo evaluation of oral salmon calcitonin-delivery system based on a thiolated chitosan carrier matrix. *Pharm. Res.* **2003**, *20*, 1989–1994.

(19) Guggi, D.; Krauland, A. H.; Bernkop-Schnurch, A. Systemic peptide delivery via the stomach: in vivo evaluation of an oral dosage form for salmon calcitonin. *J. Controlled Release* **2003**, *92*, 125–135.

(20) Krezel, A.; Bal, W. Structure–function relationships in glutathione and its analogues. *Org. Biomol. Chem.* **2003**, *1*, 3885–3890.

(21) Takeuchi, H.; Yamamoto, H.; Kawachima, Y. Mucoadhesive nanoparticulate systems for peptide drug delivery. *Adv. Drug Delivery. Rev.* **2001**, *47*, 39–54.

(22) Kafedjiiski, K.; Foger, F.; Werle, M.; Bernkop-Schnurch, A. Synthesis and in vitro evaluation of a novel chitosan–glutathione conjugate. *Pharm. Res.* **2005**, *22*, 1480–1488.

(23) Jang, K. I.; Lee, H. G. Stability of chitosan nanoparticles for L-ascorbic acid during heat treatment in aqueous solution. *J. Agric. Food Chem.* **2008**, *56*, 1936–1941.

(24) Bernkop-Schnurch, A.; Schwarz, V.; Steininger, S. Polymers with thiol groups: a new generation of mucoadhesive polymers. *Pharm. Res.* **1999**, *16*, 876–881.

(25) Guggi, D.; Bernkop-Schnurch, A. Improved paracellular uptake by the combination of different types of permeation enhancers. *J. Pharm.* **2005**, *288*, 141–150.

(26) Akhlaghi, S. P.; Saremi, S.; Ostad, S. N.; Dinarvand, R.; Atyabi, F. Discriminated effects of thiolated chitosan-coated pMMA paclitaxel-loaded nanoparticles on different normal and cancer cell lines. *Nanomed. Nanotechnol. Biol. Med.* **2010**, *6*, 689–697.

(27) Vandenberg, G. W.; Drolet, C.; Scott, S. L.; Nöue, J. D. Factors affecting protein release from alginate-chitosan coacervate microcapsules during production and gastric/intestinal simulation. *J. Controlled Release* **2001**, *77*, 297–307.

(28) Alsarra, I. A.; Neau, S. H.; Howard, M. A. Effects of preparative parameters on the properties of chitosan hydrogel beads containing *Candida rugosa* lipase. *Biomaterials* **2004**, *25*, 2645–2655.

(29) Liu, H.; Gao, C. Preparation and properties of ionically cross-linked chitosan nanoparticles. *Polym. Adv. Technol.* **2009**, *20*, 613–619.

(30) Du, J.; Zhang, S.; Sun, R.; Zhang, L. F.; Xiong, C. D.; Peng, Y. X. Novel polyelectrolyte carboxymethyl konjac glucomannan-chitosan nanoparticles for drug delivery. II. Release of albumin in vitro. *J. Biomed. Mater. Res. Part B: Appl. Biomater.* **2005**, *72B*, 299–304.

(31) Gan, Q.; Wang, T. Chitosan nanoparticles as protein delivery carrier-systematic examination of fabrication conditions for efficient loading and release. *Colloid Surf. B* **2007**, *59*, 24–34.

(32) Hornof, M. D.; Kast, C. E.; Bernkop-Schnurch, A. In vitro evaluation of the viscoelastic properties of chitosan-thioglycolic acid conjugates. *J. Pharm. Biopharm.* **2003**, *55*, 185–190.

(33) Kast, C. E.; Bernkop-Schnurch, A. Thiolated polymers – thiomers: development and in vitro evaluation of chitosan thioglycolic acid conjugates. *Biomaterials* **2001**, *22*, 2345–2352.